FEBS Letters 584 (2010) 4247–4252

FEBS Letters

journal homepage: www.FEBSLetters.org

Truncation of subunit ND2 disrupts the threefold symmetry of the antiporter-like subunits in complex I from higher metazoans

James A. Birrell, Judy Hirst *

Medical Research Council Mitochondrial Biology Unit, Wellcome Trust/MRC Building, Hills Road, Cambridge CB2 0XY, UK

ARTICLE INFO

Article history:
Received 7 September 2010
Accepted 9 September 2010
Available online 17 September 2010

Edited by Peter Brzezinski

Keywords:
Complex I
Mitochondria
Mrp antiporter
NADH:ubiquinone oxidoreductase
ND2 subunit
Proton translocation

ABSTRACT

Three of the conserved, membrane-bound subunits in NADH:ubiquinone oxidoreductase (complex I) are related to one another, and to Mrp sodium-proton antiporters. Recent structural analysis of two prokaryotic complexes I revealed that the three subunits each contain fourteen transmembrane helices that overlay in structural alignments: the translocation of three protons may be coordinated by a lateral helix connecting them together (Efremov, R.G., Baradaran, R. and Sazanov, L.A. (2010). The architecture of respiratory complex I. Nature 465, 441–447). Here, we show that in higher metazoans the threefold symmetry is broken by the loss of three helices from subunit ND2; possible implications for the mechanism of proton translocation are discussed.

1. Introduction

Complex I (NADH:ubiquinone oxidoreductase) is a major entry point for electrons to the respiratory chains of many aerobically respiring organisms. It oxidizes NADH in the mitochondrial matrix or bacterial cytosol, reduces quinone in the inner mitochondrial or cytosolic membrane, and conserves the potential energy as a proton-motive force. It is generally accepted that complex I transfers four protons across the membrane for each NADH oxidized [1–4]. Although the mechanisms of NADH oxidation and intramolecular electron transfer in complex I are increasingly well defined (reviewed in Ref. [5]), the mechanisms of ubiquinone reduction and proton translocation remain unclear.

The membrane domain of all complexes I contain seven 'core' subunits, and a varying set of supernumerary subunits are present also in higher organisms [6,7]. Three of the core subunits (ND2/Nqo14/NuoN, ND4/Nqo13/NuoM and ND5/Nqo12/NuoL) are related to one another [8], and also to proteins from the Mrp family of antiporters [9]. Thus, they have been proposed to function in proton translocation. Recently, the positions of the 55 transmembrane helices (TMHs) in complex I from *Thermus thermophilus* were modeled to electron density at 3.9 Å resolution [10]. Three matching sets of 14 TMHs, that overlay in structural alignments, were identified (see Fig. 1) [10]. The 14-helix unit comprises an external ring of helices surrounding a central core, suggestive of a function in membrane transport, and each unit includes two discontinuous or 'broken' helices, as observed previously in several transporter and channel proteins [11]. The assignment of the three 14-helix units to Nqo14, Nqo13 and Nqo12 is consistent with their expected similarity, with the lengths of the sequences in *T. thermophilus*, and with previous data that suggested that Nqo13 and Nqo12 are located towards the distal end of the hydrophobic domain [12]. An unexpected additional feature revealed by the structure is that the C-terminus of the most distal subunit (Nqo12) runs back along the protein, in a long helical structure that 'connects' the units together, perhaps to coordinate proton translocation [10]. A similar, though not identical, architecture of the membrane-bound subunits has now been observed in the electron density map for complex I from *Yarrowia lipolytica*: the lateral helical structure is present but perhaps truncated, and the membrane domain is described as two modules (ND2 is in the 'N' module, ND4 and 5 are in the 'P' module) [13].

The sequence and structural relationships between the ND2/Nqo14/NuoN, ND4/Nqo13/NuoM and ND5/Nqo12/NuoL subunits were crucial for assigning the helical patterns observed in the hydrophobic domain of *T. thermophilus* complex I, and their conserved structures support a conserved role in proton translocation [10]. However, comparison of the sequences of the ND2, ND4 and ND5 subunits from *Bos taurus* complex I [8,14] with those of the Nqo14, Nqo13 and Nqo12 subunits from *T. thermophilus*,

Abbreviation: TMH, transmembrane helix

* Corresponding author. Fax: +44 1223 252705.
E-mail address: jh@mrc-mbu.cam.ac.uk (J. Hirst).

0014-5793/$36.00
doi:10.1016/j.febslet.2010.09.017

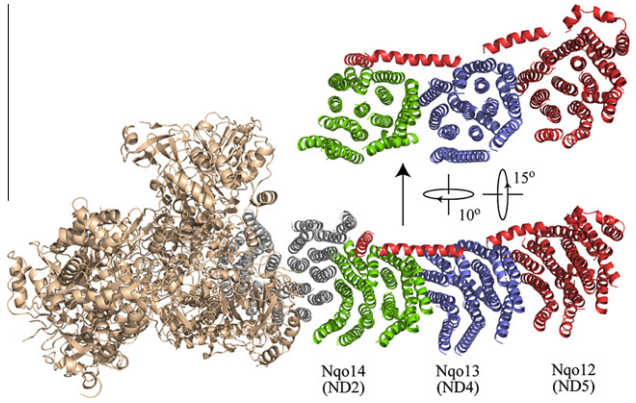

Fig. 1. The three related 14-helix subunits in the membrane domain of *T. thermophilus* complex I. The helices are green (Nqo14, fourteen helices), blue (Nqo13, fourteen helices), red (Nqo12, fourteen helices plus C-terminal extension) and grey (Nqo 7, 8, 10, 11), with the hydrophilic domain (gold) protruding from the page. The molecule is viewed from above the membrane, showing that the helices in Nqo12, 13 and 14 are tilted. Shown above the main structure are the structures of Nqo12, 13 and 14, rotated to display more clearly their structure and similarity. Taken from 3I9V.pdb [10].

immediately revealed to us that the *B. taurus* ND2 subunit is significantly shorter than its bacterial counterpart: indeed, it is not long enough to comprise fourteen THMs. The mass of the mature *B. taurus* ND2 subunit has been confirmed by mass spectrometry [15]. Here, we use sequence analyses to determine the structural extent and evolutionary origin of the truncation of ND2, and discuss possible implications for our understanding of the catalytic mechanism of complex I.

2. Methods

418 sequences for the ND2 subunit of complex I were identified in the UniProtKB database by searching for entries with the gene names nd2, nad2, nuon or nqo14, and excluding sequences that were annotated as fragments or shorter than 200 amino acids. The UniProtKB database is a manually annotated, reviewed, non-redundant protein sequence database (http://www.uniprot.org). The 418 sequences were used to create initial sequence alignments using both ClustalW [16] and MUSCLE [17]; the results were similar, and the alignments from ClustalW were imported into JalView [18]. Then, a subset of 40 sequences, that represented the phylogenetic tree most comprehensively, were chosen. Those sequences that are predicted to be 'short' sequences were verified by inspecting the nucleotide sequences upstream of the suggested initiation codons (see text). Mitochondrial genomic sequences were translated using the EMBOSS Transeq program [19]; the appropriate mitochondrial genetic code (translation table) for each species was taken from the Codon Usage Database (http://www.kazusa.or.jp/codon) [20]. The 40-sequence alignment was adjusted manually in JalView, using the Zappo representation (residues colored according to their chemical properties), Jalview sequence conservation setting, and the JalView TMH prediction function (based on HMMTOP (Hidden Markov Model for TOpology Prediction) [21]). Additional ND2 sequences for a number of basal metazoans (from the Placozoa, Porifera and Cnidaria) were derived from their mitochondrial genome sequences in the NCBI database. Forty-sequence alignments for the ND1, ND3, ND4, ND4L, ND5 and ND6 were generated similarly. For illustrative purposes, simple phylogenetic trees were constructed, based primarily on the taxonomic information available in the NCBI database (http://www.ncbi.nlm.nih.gov/), with the phylogeny of the protostomia amended according to Telford et al. [22].

3. Results and discussion

3.1. Sequence alignment for ND2 and identification of two classes of sequence

Fig. 2 presents an alignment of the ND2 subunits from six representative species, from different branches of the phylogenetic tree. *Caenorhabditis elegans*, a nematode, is a lower metazoan; *B. taurus*, the domestic cow, is a higher metazoan. The ND2 sequences from *C. elegans* and *B. taurus* are significantly shorter than the sequences from *T. thermophilus* (a bacterium), *Y. lipolytica* (a fungus), *Chondrus cripus* (a marine algae) and *Arabidopsis thaliana* (a flowering plant). The alignment in Fig. 2 is an abridged version of the 40-sequence alignment in Supplementary Fig. 1 that shows how all the sequences fall cleanly into two discrete categories, here referred to as 'long' and 'short' sequences. The short sequences are truncated by around 100 residues at the N-terminus, approximately 20% of the length of the long sequences. Furthermore, inspection of an alignment of the 418 ND2 sequences that could be identified in the UniProtKB database (comprising 245 prokaryotic and 173 eukaryotic sequences) did not reveal any sequences that do not fit into either class.

The programme HMMTOP (see Section 2 [21]) was used to predict the positions of the TMHs for each of the 40 sequences individually; the complete set of predictions is shown in Supplementary Fig. 2. The TMH predictions for each protein are mostly in agreement, but there are some discrepancies (typically a small difference in sequence produces more significant changes in the TMH prediction), indicating that considering only a single sequence might produce a misleading picture. Consequently, the number of sequences for which a helix was predicted was counted for each alignment position, and used to produce the color-density bar shown under the alignment in Fig. 2. The bar is white if there are no predicted helices at the given position, black if all the sequences have a predicted helix, and graded evenly in grey for all intermediate cases. A total of fourteen TMHs are clearly identified, consistent with structural models from *T. thermophilus* complex I and the membrane domain of *Escherichia coli* complex I [10], and with previous predictions [9,23]; only helix V is slightly ambiguous: it is the least strongly predicted, and not clearly distinct from helix IV. Importantly, Fig. 2 shows that the short sequences contain only eleven helices; the first three helices of the long 14-helix sequences are absent.

3.2. Phylogenetic analysis of the truncation of ND2

Fig. 3A shows the 40 organisms from the large sequence alignment of Supplementary Figs. 1 and 2 on a phylogenetic tree, colored according to whether they have long or short ND2 subunits. The short sequences are all from metazoans; all non-metazoan sequences, including those from prokaryotes, fungi, and plants, are long. The outlier, in Fig. 3A, is *Metridium senile*, a sea anemone and a metazoan. Originally, the sequence of *M. senile* ND2 was annotated as a short sequence, by reference to the sequences from *Mus musculus* and *Drosophila yakuba* [24]. However, our inspection of the *M. senile* mitochondrial genome sequence revealed an in-frame upstream initiator codon that yields an amino acid sequence with similarity to the N-terminal regions of the long sequences (see Supplementary Fig. 1). Therefore, the *M. senile* sequence was classified here as a long sequence. This observation indicates that a larger subset of metazoan species probably have long ND2 subunits also. Sequences from four metazoan subgroups were inspected (see Fig. 3B): 10 sequences from the Porifera and four from the Placozoa are all annotated as long sequences; 40 sequences from the Bilateria are all short; 18 sequences from the

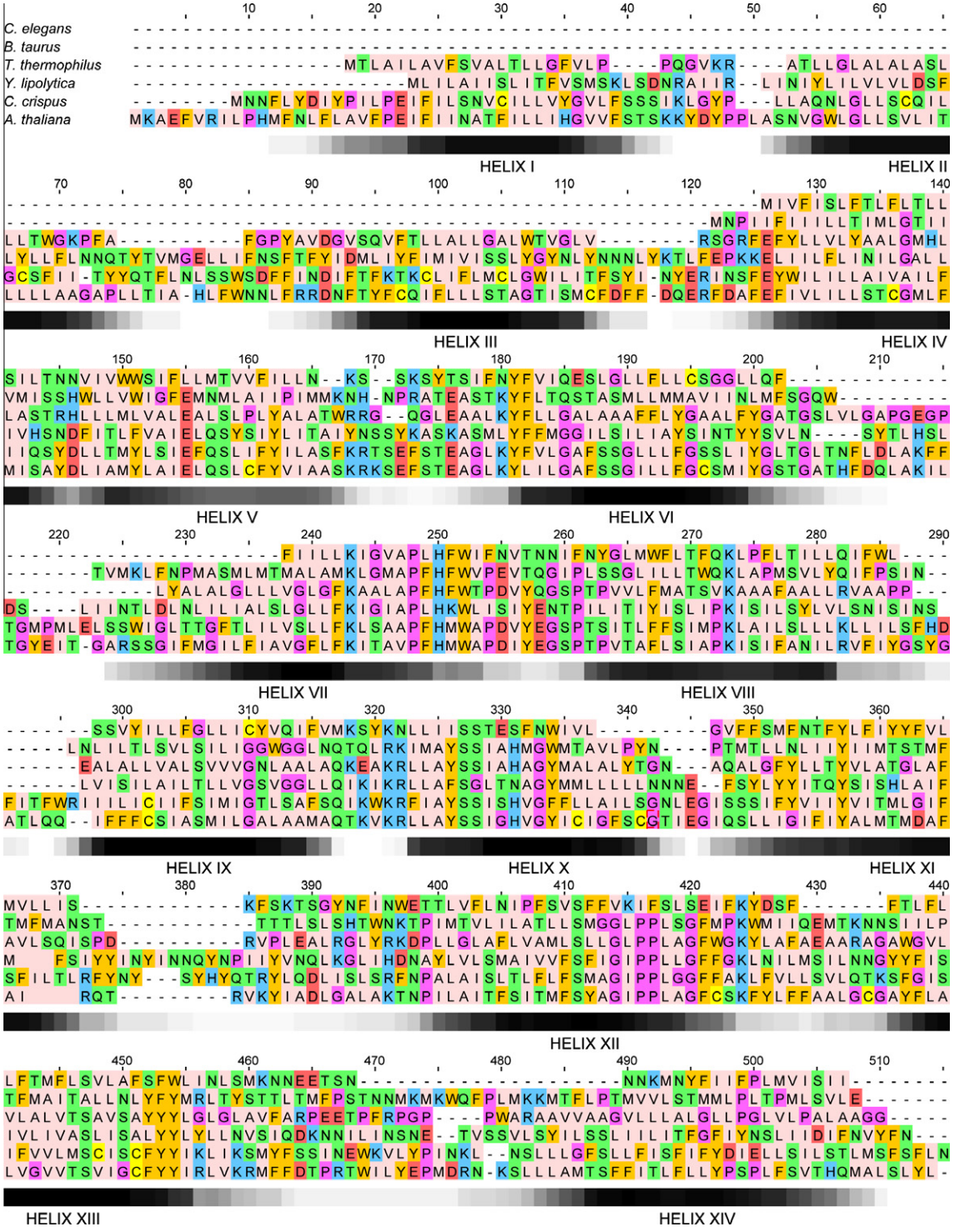

Fig. 2. Alignment of the ND2/Nqo14/NuoN subunits from six organisms, and the positions of the transmembrane helices. The residues are colored according to their chemical properties. The positions of the TMHs (I to XIV) are shown by the color-density bar, representing the number of species in the 40-species alignment (see text) for which a helix was predicted (white: no helix prediction; black: helix predicted in all sequences).

Cnidaria are a mixture of long and short. Variation in the length of ND2 within the Cnidaria has been noted previously [25–28]. Following our reclassification of the *M. senile* sequence, the cnidarian mitochondrial genome sequences were inspected. Every 'short' cnidarian sequence has an in-frame upstream initiator codon that yields an amino acid sequence with similarity to the N-terminal region of the 'long' cnidarian sequences. In contrast, when the bilaterian mitochondrial genome sequences were inspected (10 platyzoans, 10 ecdysozoans and 20 deuterostomes) a terminator codon was identified in every case, just upstream of the short-sequence initiator codon. Thus, it is likely that the cnidarian ND2 sequences are long, but we cannot rule out that some (or all) cnidarians use the downstream initiator codon to produce a short ND2. The classification in Fig. 3B is based on the position of the most-upstream initiator codon possible; our evaluation suggests that the short ND2 sequence emerged in a metazoan lineage that

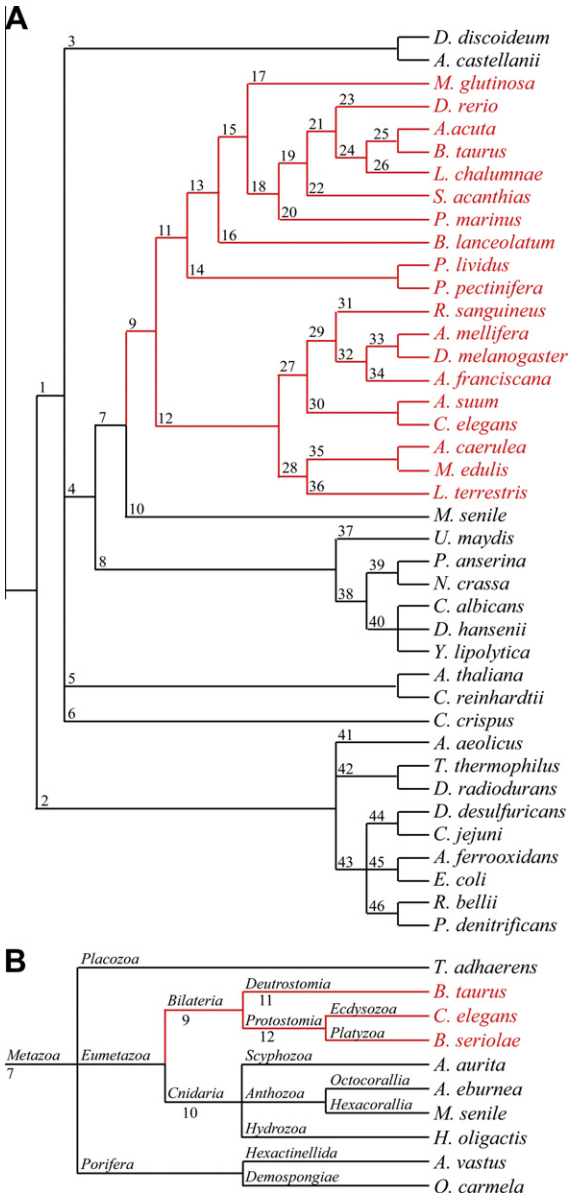

Fig. 3. Phylogenetic representation of the distribution of the short ND2 sequence. (A) The relationships between 40 organisms that encode complex I, chosen to represent as much of the phylogenetic tree as possible; black, long ND2 sequences; red, short ND2 sequences. (B) Within metazoans, the short ND2 sequence occurs only in bilateria. The lengths of the lines are illustrative only. Species: *Dictyostelium discoideum*, *Acanthamoeba castellanii*, *Myxine glutinosa*, *Danio rerio*, *Anas acuta*, *Bos taurus*, *Latimeria chalumnae*, *Squalus acanthias*, *Petromyzon marinus*, *Branchiostoma lanceolatum*, *Paracentrotus lividus*, *Patiria pectinifera*, *Rhipicephalus sanguineus*, *Apis mellifera*, *Drosophila melanogaster*, *Artemia franciscana*, *Ascaris suum*, *Caenorhabditis elegans*, *Albinaria caerulea*, *Mytilus edulis*, *Lumbricus terrestris*, *Metridium senile*, *Ustilago maydis*, *Podaspora anserina*, *Neurospora crassa*, *Candida albicans*, *Debaryomyces hansenii*, *Yarrowia lipolytica*, *Arabidopsis thaliana*, *Chlamydomonas reinhardtii*, *Chondrus crispus*, *Aquifex aeolicus*, *Thermus thermophilus*, *Deinococcus radiodurans*, *Desulfovibrio desulfuricans*, *Campylobacter jejuni*, *Acidithiobacillus ferrooxidans*, *Escherichia coli*, *Rickettsia bellii*, *Paracoccus denitrificans*, *Trichoplax adhaerens*, *Benedenia seriolae*, *Aurelia aurita*, *Ancilla eburnea*, *Hydra oligactis*, *Aphrocallistes vastus*, *Oscarella carmela*. Key to panel A: (1) Eukaryota, (2) Bacteria, (3) Amoebozoa, (4) Fungi/Metazoa, (5) Viridiplantae, (6) Rhodophyta, (7) Metazoa, (8) Fungi, (9) Bilateria, (10) Cnidaria, (11) Deuterostomia, (12) Protostomia, (13) Chordata, (14) Echinodermata, (15) Craniata, (16) Cephalochordata, (17) Hyperotreti, (18) Vertebrata, (19) Gnathostomata, (20) Hyperoartia, (21) Teleostomi, (22) Chondrichthyes, (23) Actinopterygii, (24) Sarcopterygii, (25) Tetrapoda, (26) Coelacanthimorpha, (27) Ecdysozoa, (28) Lophotrochozoa, (29) Panarthropoda, (30) Nematoida, (31) Chelicerta, (32) Mandibulata, (33) Hexapoda, (34) Crustacea, (35) Mollusca, (36) Annelida, (37) Basidiomycota, (38) Ascomycota, (39) Pezizomycotina, (40) Saccharomycotina, (41) Aquificae, (42) Deinococcus-Thermus, (43) Proteobacteria, (44) Delta/Epsilon subdivisions, (45) Gammaproteobacteria, (46) Alphaproteobacteria.

directly gave rise to bilaterian animals. Finally, we note that analyzing the phylogenetic relationships between closely related organisms using their mitochondrial DNA and protein sequences has become commonplace; analyses of the phylogenetic relationships amongst Cnidaria based on these approaches (see for example [25–28]) may have been influenced by discrepancies in the predicted lengths of ND2.

The mitochondrial genetic code varies between different branches of Metazoa, suggesting that a change in code could have truncated ND2, either by introducing a termination codon, or eliminating an initiation codon. According to the Codon Usage Database (see Section 2) Cnidaria, Porifera and Placozoa use translation Tables 4 and 5 (the 'mold, protozoan, and coelenterate' and 'invertebrate' mitochondrial codes), while Bilateria use Tables 2 (vertebrates), 5 (invertebrates) 9 (echinoderms and flatworms), 13 (ascidians) 14 (flatworms), and 21 (trematodes). The termination-codon hypothesis does not hold, because the stop codons are conserved (except code 2 has two extra stop codons and code 14 has one less). Furthermore, inspection of the placozoan and poriferan ND2 nucleotide sequences collected here showed that the common initiation codons are ATG and GTG; ATG is conserved completely, and there are known examples of GTG as an initiator in codes 2, 4, 5 and 13. Thus, we find no evidence for a change in mitochondrial code as a driver for the truncation of ND2. Alternatively, comparisons of the mitochondrial genomes of a range of metazoa have revealed mass re-organizations: the orders of the protein coding sequences and tRNAs vary between even closely related organisms, particularly between basal metazoans [24,25,28–30]. Such re-organizations could have facilitated the truncation of ND2.

3.3. Changes in protein composition that may compensate for the truncation of ND2

Multiple sequence alignments were generated for the ND1, ND3, ND4, ND4L, ND5 and ND6 subunits, using the sequences from the 40 organisms presented in Fig. 3A. Then, the programme HMMTOP (see Section 2 [21]) was used to predict the positions of the TMHs for each individual sequence, and a consensus pattern (as presented in Fig. 2 for ND2) was generated for each subunit (see Fig. S3). Clear consenuses were achieved for all the subunits, and, for each subunit, the number of predicted TMHs is consistent with recent structural information [10]. A small number of sequences are extended at their N or C terminii, or have insertions (a total of 19 extra TMHs in 240 sequences, see Fig. S3) but these extensions are all in species with long ND2 subunits. Thus, our analyses indicate that the three helices trucated from ND2 are not contributed by a different mitochondrial-encoded protein. Interestingly, two related fungal ND5 sequences appear to be truncated by two TMHs at their N-terminii (see Fig. S3), but the lengths of these subunits have been interpreted from genomic data, and not experimentally verified.

Alternatively, the three missing helices could be contributed by nuclear-encoded proteins. However, blast searches of the N-terminal sequences (comprising the first three TMHs) of the ND2 subunits from the seven placozoan, cnidarian and poriferan species in Fig. 3B, against all bilaterian sequence data available in the NCBI, failed to identify any candidate proteins. In addition, specific sequence comparisons of the known supernumerary subunits of *B. taurus* complex I [7] with these N-terminal sequences revealed no similarity. Finally, phylogenetic analyses of the subunit composition of eukaryotic complex I suggested that a number of supernumerary subunits are specific to higher metazoans [31]: if the presence of any of these subunits correlates with the truncation of ND2 then they may substitute structurally, if not functionally, for the deleted helices. Comparison of the well-defined subunit

compositions of *B. taurus* and *Y. lipolytica* [7,32,33] identified nine *B. taurus* subunits that have no homologues in *Y. lipolytica*; four of them (subunits KFYI, MLRQ, SGDH, and B14.5b) are predicted to contain TMHs [7]. Thus, the sequences of these four subunits were compared, using blast searches, to extant sequence data from all the eukaryotes shown in Fig. 3A and to data from the Placazoa, Cnideria and Porifera. No homologues to the *B. taurus* KFYI subunit were identified. Homologues to MLRQ were identified in *Danio rerio*, *Rhipicephalus sanguineus*, *Apis mellifera*, *Drosophila melanogaster* (short ND2) and in *Ustilago maydis*, *Nematostella vectensis* (Cnidaria, Hexacorallia), and *Hydra magnipapillala* (Cnidaria, Hydrozoa) (long ND2). Homolgoues to SGDH were identified in *D. rerio*, *A. mellifera*, *D. melanogaster* and *C. elegans* (short ND2). Homologues to B14.5b were identified in *D. rerio*, *A. mellifera*, and *D. melanogaster,* and have been identified previously in *C. elegans* [31] and *Neurospora crassa* (long ND2) also [33]. Thus, it is unlikely that KFYI compensates for the trucation of ND2; the three other subunits all contain only one TMH each and cannot be unambiguously ruled either in or out as candidates.

3.4. Possible implications for the mechanism of complex I

If we assume that the three N-terminal helices of ND2 are not substituted, functionally, by a different protein in complex I from higher eukaryotes then there are three possibilities: (i) ND2 is not involved in proton translocation by any complex I; (ii) the function of ND2 is not affected by the N-terminal truncation and it is involved equally in proton translocation by all complexes I; (iii) the function of ND2 is affected by the N-terminal truncation, so its function is amended in the complexes I of higher metazoans.

Recent structural models of the membrane domains of the complexes I from *E. coli*, *T. thermophilus* [10] and *Y. lipolytica* [13] (all of which contain long ND2 proteins) provide three indications that ND2 is important in proton translocation, and suggest that possibility (i) is unlikely to be correct. First, ND2 'anchors' the lateral helix comprising the C-terminus of subunit ND5. Second, like subunits ND4 and ND5, ND2 displays the characteristics of a transporter protein (a 'ring-type' helical arrangement, and two 'broken' helices, although the positions of the broken helices are not yet certain). Third, like subunits ND4 and ND5, ND2 contains two residues, a glutamate residue in helix V and a lysine residue in helix VII, that are widely conserved in complex I and in the MrpA and MrpD subunits of the related antiporters [9]. Both residues are clearly apparent in Fig. 2 (positions 155 and 243) and Supplementary Fig. 1 (positions 201 and 302) although the helix V glutamate that is present in 38 of the 40 species aligned in Supplementary Fig. 1 is absent in *C. elegans* and *Ascaris suum*, and there is an additional, fully conserved lysine in helix VIII (Fig. 2 position 273 and Supplementary Fig. 1 position 332). It is possible that these residues represent buried charges and correspond to the 'broken' helices observed in the structural models, and that they are functionally important. A single study of mutations to ND2 in *E. coli* reported decreased rates of NADH oxidation and proton translocation for the two lysines in helices VII and VIII, and lesser effects from the glutamate in helix V, but none of the mutations studied abolished catalysis, and their effects could be due to decreased protein stability [23].

It is easier to imagine (possibility ii) that a truncated ND2 is able to continue in a 'supporting role', than to imagine that three helices may be lost from the transporter unit without some effect on proton translocation. Possible supporting roles include anchoring the lateral helix and promoting the coupling of proton and electron translocation, and ND2 has been suggested to bind ubiquinone also [23,34]. It is interesting to note that both the operation of the 'active–deactive transition' in complex I from higher metazoans, and the high affinity of these enzymes for rotenone [35,36], may be related to the truncation of ND2, although there is insufficient extant data for a definitive correlation to be drawn at present.

Alternatively (possibility iii), it is tempting to speculate that the truncation of ND2 'inactivated' proton translocation through the ND2 subunit, and provoked a change of the proton-to-electron stoichiometry of complex I: the obvious interpretation would be that the complex I of higher metazoans pumps fewer protons per NADH than the fungal or bacterial enzymes. The majority of stoichiometry measurements have been carried out on the mammalian enzyme (see, for example [1–3]) for which the four-protons-per-NADH stoichiometry is relatively well established: it is possible that mammalian complexes I pump two protons per catalytic half cycle (one through subunit ND4 and one through ND5), whereas fungal and bacterial complexes I may pump three (through subunits ND4, ND5 and ND2). Whether ND2 is directly active in proton translocation is thus a key fact in distinguishing extant mechanistic models for proton translocation by complex I (for example, [10,34]). Interestingly, it has been found recently that the c-ring of ATP synthase contains only eight subunits in vertebrates, and probably in many invertebrates, but between 10 and 15 subunits in fungi and eubacteria [37]. Thus, decreases in the proton-stoichiometries of both ATP synthase and complex I may have occurred at similar points in evolution, perhaps in response to evolutionary pressure to maintain the NADH to ATP ratio.

Acknowledgements

We thank Alan J. Robinson for advice on bioinformatic analyses. This research was funded by The Medical Research Council.

Appendix A. Supplementary data

Supplementary data associated with this article can be found, in the online version, at doi:10.1016/j.febslet.2010.09.017.

References

[1] Wikström, M. (1984) Two protons are pumped from the mitochondrial matrix per electron transferred between NADH and ubiquinone. FEBS Lett. 169, 300–304.
[2] Galkin, A.S., Grivennikova, V.G. and Vinogradov, A.D. (1999) $H^+/2e^-$ stoichiometry in NADH-quinone reductase reactions catalyzed by bovine heart submitochondrial particles. FEBS Lett. 451, 157–161.
[3] Hinkle, P.C. (2005) P/O ratios of mitochondrial oxidative phosphorylation. Biochim. Biophys. Acta 1706, 1–11.
[4] Galkin, A.S., Dröse, S. and Brandt, U. (2006) The proton pumping stoichiometry of purified mitochondrial complex I reconstituted into proteoliposomes. Biochim. Biophys. Acta 1757, 1575–1581.
[5] Hirst, J. (2010) Towards the molecular mechanism of respiratory complex I. Biochem. J. 425, 327–339.
[6] Walker, J.E. (1992) The NADH-ubiquinone oxidoreductase (complex I) of respiratory chains. Q. Rev. Biophys. 25, 253–324.
[7] Hirst, J., Carroll, J., Fearnley, I.M., Shannon, R.J. and Walker, J.E. (2003) The nuclear encoded subunits of complex I from bovine heart mitochondria. Biochim. Biophys. Acta 1604, 135–150.
[8] Fearnley, I.M. and Walker, J.E. (1992) Conservation of sequences of subunits of mitochondrial complex I and their relationships with other proteins. Biochim. Biophys. Acta 1140, 105–134.
[9] Mathiesen, C. and Hägerhäll, C. (2002) Transmembrane topology of the NuoL, M and N subunits of NADH:quinone oxidoreductase and their homologues among membrane-bound hydrogenases and bona fide antiporters. Biochim. Biophys. Acta 1556, 121–132.
[10] Efremov, R.G., Baradaran, R. and Sazanov, L.A. (2010) The architecture of respiratory complex I. Nature 465, 441–447.
[11] Screpanti, E. and Hunte, C. (2007) Discontinuous membrane helices in transport proteins and their correlation with function. J. Struct. Biol. 159, 261–267.
[12] Baranova, E.A., Morgan, D.J. and Sazanov, L.A. (2007) Single particle analysis confirms distal location of subunits NuoL and NuoM in *Escherichia coli* complex I. J. Struct. Biol. 159, 238–242.
[13] Hunte, C., Zickermann, V. and Brandt, U. (2010) Functional modules and structural basis of conformational coupling in mitochondrial complex I. Science 329, 448–451.

[14] Chomyn, A. et al. (1985) Six unidentified reading frames of human mitochondrial DNA encode components of the respiratory-chain NADH dehydrogenase. Nature 314, 592–597.
[15] Carroll, J., Fearnley, I.M. and Walker, J.E. (2006) Definition of the mitochondrial proteome by measurement of molecular masses of membrane proteins. Proc. Natl. Acad. Sci. USA 103, 16170–16175.
[16] Thompson, J.D., Higgins, D.G. and Gibson, T.J. (1994) CLUSTAL W: improving the sensitivity of progressive multiple sequence alignment through sequence weighting, position-specific gap penalties and weight matrix choice. Nucleic Acids Res. 22, 4673–4680.
[17] Edgar, R.C. (2004) MUSCLE: multiple sequence alignment with high accuracy and high throughput. Nucleic Acids Res. 32, 1792–1797.
[18] Waterhouse, A.M., Procter, J.B., Martin, D.M.A., Clamp, M. and Barton, G.J. (2009) Jalview Version 2 – a multiple sequence alignment editor and analysis workbench. Bioinformatics 25, 1189–1191.
[19] Rice, P., Longden, I. and Bleasby, A. (2000) EMBOSS: the European molecular biology open software suite. Trends Genet. 16, 276–277.
[20] Nakamura, Y., Gojobori, T. and Ikemura, T. (2000) Codon usage tabulated from international DNA sequence databases: status for the year 2000. Nucleic Acids Res. 28, 292.
[21] Tusnády, G.E. and Simon, I. (1998) Principles governing amino acid composition of integral membrane proteins: application to topology prediction. J. Mol. Biol. 283, 489–506.
[22] Telford, M.J., Bourlat, S.J., Economou, A., Papillon, D. and Rota-Stabelli, O. (2008) The evolution of the ecdysozoa. Philos. Trans. R. Soc. B 363, 1529–1537.
[23] Amarneh, B. and Vik, S.B. (2003) Mutagenesis of subunit N of the *Escherichia coli* complex I. Identification of the initiation codon and the sensitivity of mutants to decylubiquinone. Biochemistry 42, 4800–4808.
[24] Beagley, C.T., Okimoto, R. and Wolstenholme, D.R. (1998) The mitochondrial genome of the sea anemone *Metridium senile* (Cnidaria): introns, a paucity of tRNA genes, and a near-standard genetic code. Genetics 148, 1091–1108.
[25] Beaton, M.J., Roger, A.J. and Cavalier-Smith, T. (1998) Sequence analysis of the mitochondrial genome of *Sarcophyton glaucum*: conserved gene order among octocorals. J. Mol. Evol. 47, 697–708.
[26] McFadden, C.S., Tullis, I.D., Hutchinson, M.B., Winner, K. and Sohm, J.A. (2004) Variation in coding (NADH dehydrogenase subunits 2, 3, and 6) and noncoding intergenic spacer regions of the mitochondrial genome in Octocorallia (Cnidaria: Anthozoa). Mar. Biotechnol. 6, 516–526.
[27] McFadden, C.S., France, S.C., Sánchez, J.A. and Alderslade, P. (2006) A molecular phylogenetic analysis of the Octocorallia (Cnidaria: Anthozoa) based on mitochondrial protein-coding sequences. Mol. Phylogenet. Evol. 41, 513–527.
[28] Brugler, M.R. and France, S.C. (2007) The complete mitochondrial genome of the black coral *Chrysopathes formosa* (Cnidaria:Anthozoa:Antipatharia) supports classification of antipatharians within the subclass Hexacorallia. Mol. Phylogenet. Evol. 42, 776–788.
[29] Ruiz-Trillo, I., Riutort, M., Fourcade, H.M., Baguña, J. and Boore, J.L. (2004) Mitochondrial genome data support the basal position of Acoelomorpha and the polyphyly of the Platyhelminthes. Mol. Phylogenet. Evol. 33, 321–332.
[30] Sinniger, F., Chevaldonné, P. and Pawlowski, J. (2007) Mitochondrial genome of *Savalia savaglia* (Cnidaria, Hexacorallia) and early metazoan phylogeny. J. Mol. Evol. 64, 196–203.
[31] Gabaldón, T., Rainey, D. and Huynen, M.A. (2005) Tracing the evolution of a large protein complex in the eukaryotes, NADH:ubiquinone oxidoreductase (complex I). J. Mol. Biol. 348, 857–870.
[32] Morgner, N. et al. (2008) Subunit mass fingerprinting of mitochondrial complex I. Biochim. Biophys. Acta 1777, 1384–1391.
[33] Huynen, M.A., de Hollander, M. and Szklarczyk, R. (2009) Mitochondrial proteome evolution and genetic disease. Biochim. Biophys. Acta 1792, 1122–1129.
[34] Ohnishi, S.T., Salerno, J.C. and Ohnishi, T. (in press). Possible roles of two quinone molecules in direct and indirect proton pumps of bovine heart NADH-quinone oxidoreductase (complex I). Biochim. Biophys. Acta.
[35] Kotlyar, A.B. and Vinogradov, A.D. (1990) Slow active/inactive transition of the mitochondrial NADH-ubiquinone reductase. Biochim. Biophys. Acta 1019, 151–158.
[36] Grivennikova, V.G., Maklashina, E.O., Gavrikova, E.V. and Vinogradov, A.D. (1997) Interaction of the mitochondrial NADH-ubiquinone reductase with rotenone as related to the enzyme active/inactive transition. Biochim. Biophys. Acta 1319, 223–232.
[37] Watt, I.N., Montgomery, M.G., Runswick, M.J., Leslie, A.G.W. and Walker, J.E. (in press). Bioenergetic cost of making and adenosine triphosphate molecule in animal mitochondria. Proc. Natl. Acad. Sci. USA.